

1 **Revealing metabolic flexibility of *Candidatus***
2 ***Accumulibacter phosphatis* through redox cofactor**
3 **analysis and metabolic network modeling**
4
5 **Running title: Metabolic flexibility of *Accumulibacter***

6 Leonor Guedes da Silva#, Karel Olavarria Gamez, Joana Castro Gomes,
7 Kasper Akkermans, Laurens Welles, Ben Abbas, Mark C.M. van Loosdrecht,
8 Sebastian Aljoscha Wahl

9
10 Department of Biotechnology, Delft University of Technology, The
11 Netherlands

12
13 #Address correspondence to Leonor Guedes da Silva,
14 LeonorGuedesdaSilva@gmail.com

15
16 These investigations were supported by the SIAM Gravitation Grant
17 024.002.002, the Netherlands Organization for Scientific Research (NWO).
18 The authors declare no conflict of interest.

19 **KEYWORDS**

20 *Candidatus* *Accumulibacter phosphatis*, Polyphosphate Accumulating
21 Organisms (PAO), Enhanced Biological Phosphate Removal (EBPR), Central
22 carbon metabolism, Redox cofactors, Flux Balance Analysis, Enzymatic assays

23 **ABSTRACT**

24 Environmental fluctuations in the availability of nutrients lead to intricate
25 metabolic strategies. *Candidatus Accumulibacter phosphatis*, a polyphosphate
26 accumulating organism (PAO) responsible for enhanced biological phosphorus
27 removal (EBPR) from wastewater treatment systems, is prevalent in
28 aerobic/anaerobic environments. While the overall metabolic traits of these
29 bacteria are well described, the inexistence of isolates has led to controversial
30 conclusions on the metabolic pathways used.

31 Here, we experimentally determined the redox cofactor preference of
32 different oxidoreductases in the central carbon metabolism of a highly enriched
33 *Ca. A. phosphatis* culture. Remarkably, we observed that the acetoacetyl-CoA
34 reductase engaged in polyhydroxyalkanoates (PHA) synthesis is NADH-
35 preferring instead of the generally assumed NADPH dependency. Based on
36 previously published meta-omics data and the results of enzymatic assays, a
37 reduced central carbon metabolic network was constructed and used for
38 simulating different metabolic operating modes. In particular, scenarios with
39 different acetate-to-glycogen consumption ratios were simulated. For a high
40 ratio (i.e. more acetate), a polyphosphate-based metabolism arises as optimal
41 with a metabolic flux through the glyoxylate shunt. In case of a low acetate-to-
42 glycogen ratio, glycolysis is used in combination with reductive branch of the
43 TCA cycle. Thus, optimal metabolic flux strategies will depend on the
44 environment (acetate uptake) and on intracellular storage compounds
45 availability (polyphosphate/glycogen).

46 This metabolic flexibility is enabled by the NADH-driven PHA synthesis. It
47 allows for maintaining metabolic activity under varying environmental substrate

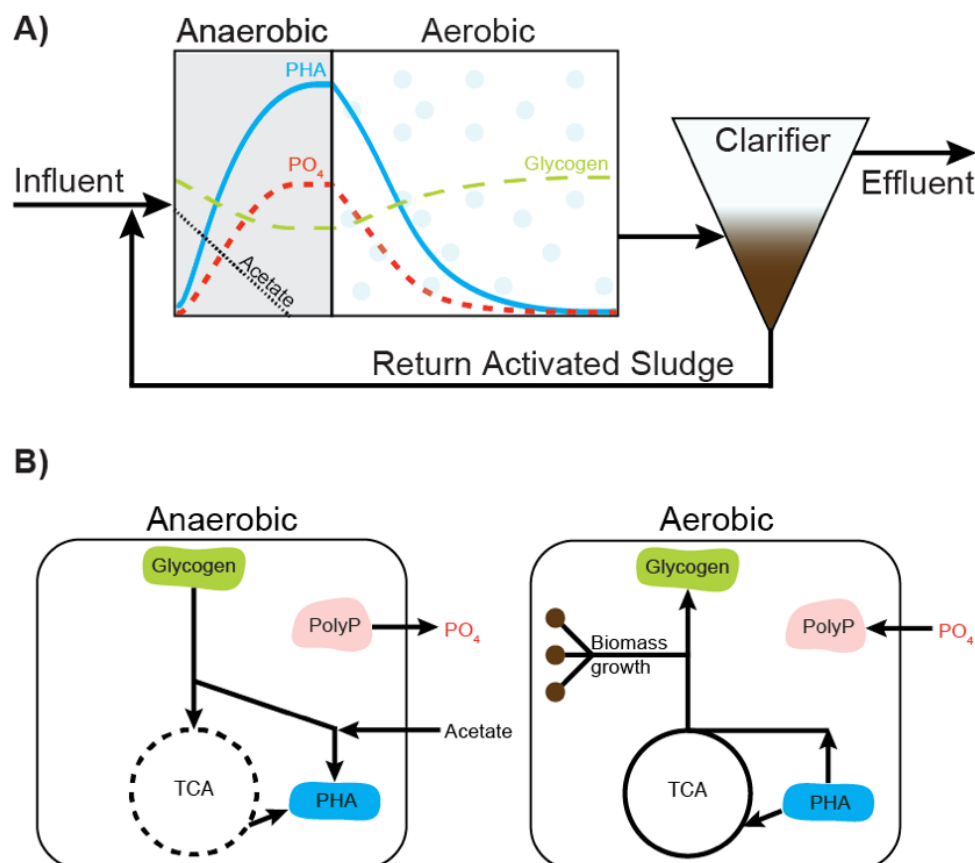
conditions, with high carbon conservation and lower energetic costs compared to NADPH dependent PHA synthesis. Such (flexible) metabolic redox coupling can explain PAOs' competitiveness under oxygen-fluctuating environments.

IMPORTANCE

Here we demonstrate how microbial metabolism can adjust to a wide range of environmental conditions. Such flexibility generates a selective advantage under fluctuating environmental conditions. It can also explain the different observations reported in PAO literature, including the capacity of *C. Accumulibacter phosphatis* to act like glycogen accumulating organisms (GAO). These observations stem from slightly different experimental conditions and controversy only arises when one assumes metabolism can only operate in one single mode. Furthermore, we also show how the study of metabolic strategies is possible when combining -omics data with functional assays and modeling. Genomic information can only provide the potential of a microorganism. The environmental context and other complementary approaches are still needed to study and predict the functional application of such metabolic potential.

65 INTRODUCTION

66 Natural habitats of microorganisms are dynamic environments with
 67 intermittent supply of nutrients. Under these dynamic conditions, organisms are
 68 selected that can accumulate growth substrates when these are abundant to
 69 compensate for periods when these are exhausted (1).



70

71 Figure 1 – Schematic diagram of an EBPR process with nutrient/polymer profiles (A) and
 72 corresponding metabolic strategy (B). Recirculated activated sludge containing PAOs is mixed
 73 with influent wastewater in an anaerobic reactor. To compensate for the absence of an external
 74 electron acceptor, Accumulibacter use their polyphosphate and glycogen reserves to take up
 75 organic carbon sources (e.g. acetate) and accumulate them in the form of
 76 polyhydroxyalkanoates (PHA). Phosphate is released at this stage. The TCA cycle is
 77 represented by a dashed line has it can have different operating modes. When oxygen
 78 becomes available, Accumulibacter makes use of their PHA storage to grow, to replenish
 79 glycogen and polyphosphate. The re-accumulation of polyphosphate in growing biomass and
 80 subsequent purge of this biomass leads to the net removal of phosphate from wastewater.
 81 Adapted from (2, 3). PHA, polyhydroxyalkanoates; PolyP, polyphosphate; PO₄, phosphate;
 82 TCA, tricarboxylic acid cycle.

Enhanced biological phosphate removal (EBPR) from wastewater is designed to make use of such physiological feature by circulating activated sludge through alternating zones with or without an external electron acceptor here respectively defined as aerobic/anaerobic (see Figure 1A) (4, 5). This environment selects for polyphosphate accumulating organisms (PAOs) like *Candidatus Accumulibacter phosphatis* (hereafter referred to as *Accumulibacter*). These bacteria thrive under these dynamic conditions thanks to a complex metabolic strategy encompassing the cycling of three common storage polymers: polyphosphate, glycogen and polyhydroxyalkanoates (PHA). Of these, polyphosphate stands out for allowing for fast and competitive harvesting of organic matter in the absence of an external electron acceptor (see Figure 1B).

In the past decades, a number of researchers have derived hypotheses about *Accumulibacter*'s (anaerobic) physiology (4, 6–8). One of the most important inconclusive discussions is the source of reducing power for the anaerobic accumulation of polyhydroxyalkanoates (PHA) from volatile fatty acids (e.g. acetate, propionate), as reviewed by Zhou *et al* (9). Most experimental approaches were adequate to study the general physiology of *Accumulibacter* species, however the inherent population heterogeneity has not yet been sufficiently addressed; for example, only recently researchers have reported different *Accumulibacter* clades showing different kinetic characteristics leading to different metabolic operations (10). Furthermore, novel meta-omics approaches were used, which allowed for *Accumulibacter*-targeted (culture-independent) analysis without the interference of other, non-*Accumulibacter*, sub-populations. A comprehensive overview of the physiological studies published on *Accumulibacter* can be found in the

Supplementary Document S1. In one of the metatranscriptomic studies (11), Oyserman and colleagues highlighted the need for validating assumptions often made in metabolic models of *Accumulibacter*. In particular, they refined the discussion on reducing power sources and requirements by making a distinction between the different redox cofactors, NADH and NADPH. This distinction imposes a constraint between sources and sinks for each redox cofactor, which can only be alleviated by energy-consuming transhydrogenase(-like) mechanisms or using electrons for hydrogen production. However, in their analysis, the specificity of the involved oxidoreductases was derived from analogy with other organisms.

In *Accumulibacter*, reducing power is required for the conversion of acetate to 3-hydroxybutyrate (3HB), the monomer of the reserve polymer poly-3-hydroxybutyrate (PHB). The intermediate reduction step is catalyzed by the enzyme acetoacetyl-CoA reductase (AAR). In PHA accumulating bacteria such as *Cupriavidus necator* and *Zoogloea ramigera*, the preferred electron donor cofactor of the AAR is NADPH (12), which was the cofactor assumed by analogy for *Accumulibacter* (11). However, AARs accepting both NADH and NADPH have been reported for *Azotobacter beijerinckii* (13, 14) and *Allochromatium vinosum* (15). A brief thermodynamic feasibility analysis of the coupling between glycolysis and either NADPH- or NADH-preferring AAR is present in the Supplementary Document S2.

So far and to our knowledge, the nature of the cofactor accepted by *Accumulibacter*'s acetoacetyl-CoA reductase has not yet been experimentally established. In this study, we addressed this knowledge gap by measuring the NADH- and NADPH-dependent acetoacetyl-CoA reductase activities in a cell free extract from a highly enriched culture of *Accumulibacter*. We further

135 extended the analysis to other key oxidoreductases involved in the anaerobic
 136 metabolism of *Accumulibacter*. These results were then used to update
 137 *Accumulibacter*'s biochemical model and as constraints in a flux balance
 138 analysis (FBA) framework. Our simulations show how the use of different
 139 pathways and storage compounds lead to metabolic flexibility. Without this
 140 flexibility, *Accumulibacter*'s metabolism would become very restrictive and,
 141 under unpredictable anaerobic environments, it could lead to situations where
 142 only a limited fraction of the available substrate could be consumed.

143 MATERIALS AND METHODS

144 Reactor operation

145 Two independent *Accumulibacter* enrichments were obtained in sequencing
146 batch reactors (SBR). The main operational conditions are described in Table
147 2 and were adapted from the SBR-S as described in Welles *et al* (10).

148 Cell free extracts preparation

149 Broth samples (10 mL) collected from the bioreactor during both anaerobic
150 and aerobic phases were centrifuged (2500g, 10 min, 4°C) and the pellet was
151 washed using 10 mL buffer (hereafter named Buffer 1X) containing 50 mM Tris
152 at pH 8, 5 mM MgCl₂, 5 mM NaCl and 5% (v/v) glycerol, and the obtained
153 suspension was centrifuged again (2500g, 10 min, 4°C). After centrifugation,
154 pellets were kept at -20°C for no longer than four days until further analysis. For
155 the enzymatic assay, cellular pellets were suspended in 10 mL of Buffer 1X
156 supplemented with 2 mM (L+D) 1,4-Dithiothreitol (DTT) and cOmplete™ mini
157 protease inhibitor cocktail (Roche). To avoid overheating and protein
158 denaturation, cells were kept on ice while being sonicated until the cell
159 suspension was homogenized (i.e. no granules visible). The resulting
160 suspension was centrifuged (15000g for at least 45 min, 4°C). The obtained
161 supernatant, a cell free extract (CFE), was used for the enzymatic assays.

162 Enzymatic assays

163 The reaction mixtures used for each enzymatic assay are described in Table
164 1. Activities were calculated using the initial rate of reduction of NAD(P)⁺ or
165 oxidation of NAD(P)H, which was obtained by following the changes in the
166 absorbance at 340 nm, at 30°C. To control the contribution of putative
167 background reactions, reaction mixtures were monitored that contained all the

168 components except one substrate or without addition of CFE (see “Controls” in
169 Supplementary Document S4). The measured rates were normalized to the
170 total protein concentration in the respective CFE. The protein concentration was
171 measured using the Bradford dye-binding protein assay (Bio-Rad), using
172 known concentrations of bovine serum albumin as external standards.

173 Table 1 – Origin of the cell free extract (CFE), buffer, substrates, controls and references
174 (16–24) used for each enzymatic assay. Controls used can be found in Supplementary
175 Document S4.

CFE	Tested enzyme	Buffer	Substrates	Reference
SBR-1	acetoacetyl-CoA reductase (AAR)	1X, supplemented	200 μ M acetoacetyl-CoA, 200 μ M NADH or 200 μ M NADPH	(16)
SBR-2	acetoacetyl-CoA reductase (AAR)	1X, supplemented	40 μ M acetoacetyl-CoA, 100 μ M NADH or 200 μ M NADPH	(17)
SBR-2	3-hydroxybutyryl-CoA dehydrogenase (3HBDH)	1X, supplemented	100 μ M 3-hydroxybutyryl-CoA 1000 μ M NAD(P) ⁺	(17)
SBR-1	glucose-6-phosphate dehydrogenase (G6PDH)	1X, supplemented	2 mM glucose-6-phosphate; 2000 μ M NAD ⁺ or 200 μ M NADP ⁺	(18)
SBR-2	glucose-6-phosphate dehydrogenase (G6PDH)	1X, supplemented	4 mM glucose-6-phosphate; 400 μ M NAD(P) ⁺	
SBR-2	isocitrate dehydrogenase (ICDH)	1X, supplemented	400 μ M NAD(P) ⁺ 400 μ M isocitrate	(19)
	malate dehydrogenase (MDH)	1X, supplemented	200 μ M NAD(P)H 200 μ M oxaloacetate	(20)
	malic enzyme (ME)	1X, supplemented	200 μ M NADP 200 μ M L-malate	(21)
	isocitrate lyase (ICL)	40 mM HEPES, pH 7, 6 mM MgCl ₂	4 mM isocitrate, 280 μ M NADH 45 units lactate dehydrogenase from rabbit muscle (Roche)	(22)
	fumarate reductase (FR)	50 mM HEPES, pH 7	15 mM fumarate 250 μ M NADH	(23)
	α -ketoglutarate dehydrogenase (AKGDH)	50 mM HEPES, pH 7, 1mM MgCl ₂ , 1mM Thiamine pyrophosphate, 2.5 mM DTT	2 mM α -ketoglutaric acid 100 μ M Coenzyme A 2.5 mM NAD(P) ⁺	(24)

176

177 **Microbial community characterization**

178 The microbial community present in our enrichments has been characterized
179 by three orthogonal approaches as described below and the detailed results
180 can be found in Supplementary Document S3.

181 Fluorescence *in situ* hybridization (FISH) was used to qualitatively assess
182 the presence of *Accumulibacter* in the enrichment cultures. All bacteria were
183 targeted by the EUB338 mix (general bacteria probe) (25–27). *Accumulibacter*
184 clade I and II were targeted by the probes Acc-1-444 and Acc-2-444 (28),
185 respectively. Hybridized samples were examined with a Zeiss Axioplan-2
186 epifluorescence microscope.

187 To further confirm the specific *Accumulibacter* clade, the presence of the
188 gene encoding for the polyphosphate kinase I (*ppk1*) present in *Accumulibacter*
189 was tested as described in (29, 30) using the primers ACCppk1-254F and
190 ACCppk1-1376R targeting the *ppk1* gene from *Accumulibacter*-like bacteria
191 (31). The *ppk1* gene sequences obtained in this study have been deposited in
192 the GenBank database under accession numbers MH899084-MH899086.

193 To identify putative side-populations, 16S-rRNA gene amplicon sequencing
194 was applied. DNA samples from cell pellets were extracted using the DNeasy
195 UltraClean Microbial Kit (Qiagen, The Netherlands). Approximately 250 mg wet
196 biomass was treated according to the standard protocol except an alternative
197 lysis was implemented. This included a combination of 5 min of heat (65°C)
198 followed by 5 min of bead-beating for cell disruption on a Mini-Beadbeater-24
199 (Biospec, U.S.A.). After extraction the DNA was checked for quality by gel
200 electrophoresis and quantified using a Qubit 4 (Thermo Fisher Scientific,
201 U.S.A.).

After quality control, samples were sent to Novogene Ltd. (Hongkong, China) for amplicon sequencing of the V3-4 region of the 16S-rRNA gene (position 341-806) on an Illumina paired-end platform. After sequencing, the raw reads were quality filtered, chimeric sequences were removed and OTUs were generated on the base of $\geq 97\%$ identity. Subsequently, microbial community analysis was performed by Novogene using Mothur & Qiime software(V1.7.0) (32, 33). For phylogenetical determination, the most recent SSURef database from SILVA (34) was used. The microbial communities in each enrichment were compared based on the 10 most abundant OTUs with a distinctive genus (i.e. with most reads assigned to it). The 16S-rRNA gene amplicon data have been deposited in GenBank under Bioproject PRJNA490689.

Anaerobic biochemical model of Accumulibacter

The metabolic network shown in Figure 2 is based on the ancestral genome reconstruction of Accumulibacter proposed by (2) as well as experimental observations obtained here. Additionally, an extensive literature overview supporting this biochemical model of Accumulibacter can be found in Supplementary Document S1.

Flux balance analysis (stoichiometric modeling)

To estimate the possible metabolic flux distributions Flux Balance Analysis (FBA) has been applied (35). The flux distribution can be obtained by optimization:

$$v_{opt} = \arg \min_v v_{CO2_{prod}} \quad \text{subject to} \quad \begin{cases} Nv = 0 \\ v_{irr} \geq 0 \\ v_{Glyc_{deg}} = 1 - f \\ v_{Ac_{upt}} = f \end{cases}$$

$$\text{with } f = 0 \dots 1 \frac{C_{mol}}{C_{mol} C_{consumed}}$$

where N is the stoichiometry matrix containing the reactions later shown in Table 3 and v is the vector containing all reaction fluxes (see also Supplementary Document S6). The simulation assumes that none of the balanced intermediates is accumulating inside the cell (steady-state assumption). This is acceptable given the long simulation period compared to the turnover time of these intermediates. Inequality constraints were introduced for physiologically irreversible fluxes (i.e. these should always be positive). The consumption of acetate and glycogen is varied between only acetate ($f = 1$) to only glycogen ($f = 0$). The respective experimental data is normalized to a summed consumption of 1 Cmol (see Supplementary Document S5).

Commonly, maximization of biomass synthesis is used in FBA as an optimization objective. However, *Accumulibacter* only grows aerobically and on the intracellular carbon reserves (PHAs) accumulated during substrate uptake in the anaerobic period. Biomass synthesis was thus assumed proportional to the carbon stored as PHA. Consequently, maximal carbon conservation in PHA, resp. minimal CO_2 production, is set as the cellular objective for the anaerobic phase.

To prevent adding a stoichiometric constraint due to an assumption on the proportion of the different PHA polymers possible, i.e. poly-3-hydroxybutyrate (PHB), poly-3-hydroxyvalerate (PHV), poly-3-hydroxy-2-methylbutyrate (PH2MB), or poly-3-hydroxy-2-methylvalerate (PH2MV), the respective monomer amount is introduced, i.e. the reduced precursors Ac-CoA* and Pr-CoA* such that:

248 $2 \text{ Ac-CoA}^* \rightarrow 3 \text{ HB};$

249 $\text{Ac-CoA}^* + \text{Pr-CoA}^* \rightarrow 3 \text{ HV (or 3H2MB)};$

250 $2 \text{ Pr-CoA}^* \rightarrow 3 \text{ H2MV};$

251 **Compilation and normalization of stoichiometric data**

252 The results of the aforementioned simulations were compared to
 253 stoichiometric data reported in literature for several different *Accumulibacter*
 254 enrichments. Anaerobic-feast yields were used when available, otherwise the
 255 yields of the whole anaerobic phase were used. In case of missing compound
 256 rates (usually CO_2 , PH2MV), these were estimated using electron and carbon
 257 balancing (see Supplementary Document S5). For datasets with redundant
 258 measurements, a data reconciliation method was applied (36). For all
 259 calculations, we assumed acetate and glycogen monomers were the only
 260 substrates and CO_2 , PHB, PHV and PH2MV were the only products. In case
 261 yields were reported without the respective error, the error was calculated using
 262 error propagation. Here, the relative errors were assumed as follows: 5% for
 263 acetate and PHB measurements, and 10% for PHV, PH2MV and glycogen
 264 measurements. From the (reconciled) rates for PHB, PHV and PH2MV, the
 265 respective Ac-CoA^* and Pr-CoA^* rates were determined and normalized to the
 266 amount of consumed substrates, in Cmol.

RESULTS

Characterization of Accumulibacter enrichments

This study was carried out using two independent Accumulibacter enrichment cultures. SBR-1 contained the highest enrichment of Accumulibacter observed in our lab. However, this cultivation was operating close to a critical dilution rate which, unfortunately, resulted in washout (i.e. enrichment deterioration) after sampling. In SBR-2, conditions were adjusted to reduce the risk of washout, i.e. higher COD load and higher SRT were used.

Table 2 – Process parameters and key performance indicators of the two independent enrichments of Accumulibacter.

	SBR-1	SBR-2	
pH	7.6	7.6	
T	20°C	20°C	
Carbon source	210 mg COD/L (63:37 Acetate:Propionate)	400 mg COD/L (75:25 Acetate:Propionate)	
Phosphate load per C	0.1 Pmol/Cmol	0.1 Pmol/Cmol	
Cycle time	6 h Settling – 76 min; Anaerobic – 135 min; Aerobic – 135 min.	6 h Settling – 30 min; Anaerobic – 112 min; Aerobic – 200 min.	
HRT	12 h	12 h	
SRT	4 days	5.6 days	
Aerobic SRT	1.5 days	3.1 days	
Anaerobic P-release per C-fed	0.58 Pmol/Cmol	~0.75 Pmol/Cmol	
Anaerobic-feast length	~41 min	~42 min	
FISH	PAO Acc I	PAO Acc I	
16S rRNA gene amplicon sequencing (dominant OTUs)	Ca_Accumulibacter Rhodopseudomonas Blastochloris	Start: Dechloromonas Ca_Accumulibacter genus from f_Hyphomonadaceae	End: Ca_Accumulibacter Chryseobacterium genus from o_Sphingobacteriales
ppk1 analysis	Dominant: clade IC	Dominant: clade IA	

For both cultures, anaerobic P-release per C-fed indicated that the PAO present in the sludge are likely saturated with polyphosphate and that glycogen accumulating organisms (GAO) are not present (37). Furthermore, microbial characterization by FISH showed *Accumulibacter* from clade I were the majority of the microorganisms across all biomass samples as it can be seen by the high overlap between the *Accumulibacter*-specific probe and the general Bacteria probe (micrographs available in Supplementary Document S3). The *ppk1* gene analysis further specified which subclade was dominant and the 16S-rRNA gene analysis provided information on the genus of the most abundant subpopulations next to *Accumulibacter* (see Table 2 and Supplementary Document S3).

Redox cofactor preferences of key oxidoreductases

For the simulation and interpretation of the metabolic network function it was essential to identify the cofactor specificity of relevant reactions. Enzymatic assays were performed using cell free extracts. While these assays cannot discriminate which organism has the respective activity, the performed assays still answer: 1) if an activity is not observed for the whole community, it is also not present in *Accumulibacter*, 2) if the cell extract shows a clear preference for NAD(H) or NADP(H) this is most probably also the preferred cofactor of *Accumulibacter* which is highly enriched in the culture.

The enzymatic activity assay results display a clear preference which is sufficient to annotate a specific cofactor. These are shown in blue in the metabolic network in Figure 2. Further details can be found in Supplementary Document S4. The different assay results will be presented from the sinks (PHA) to the putative sources of reducing power:

(1) Redox cofactor preference (NADH or NADPH) of the PHA synthesis. The CFE from SBR-1 had a NADH preferring acetoacetyl-CoA reductase. The activity was 10x higher with NADH compared to NADPH as substrate. To further confirm this cofactor preference, the acetoacetyl-CoA reductase activity was assayed using CFEs from a second enrichment (SBR-2) and both directions of the reaction were monitored (i.e. $\text{NAD(P)H} + \text{acetoacetyl-CoA} \leftrightarrow \text{NAD(P)}^+ + 3\text{-hydroxybutyryl-CoA}$).

(2) Stoichiometry of glycolysis – Embden-Meyerhof-Parnas (EMP) or Entner-Doudoroff (ED)? To discriminate between these pathways, the presence of the glucose-6-phosphate dehydrogenase, the enzyme that catalyzes the first step of ED was measured. This reaction is also common to the oxidative branch of the pentose phosphate pathway (oxPP). No activity was found in the CFEs from both SBRs. The biological positive control, a CFE from *P. putida* KT2440, showed activity with both NAD^+ and NADP^+ , as expected (38). Therefore, *Accumulibacter* nor the community have an active ED or oxPP pathway leaving EMP as glycolytic route.

(3) Alternative NADPH sources. For many organisms oxPP is an important source of NADPH for growth (20). This activity was not found in *Accumulibacter*, raising the question if NADPH could be provided by other reaction like isocitrate dehydrogenase. The oxidation of isocitrate was tested using either NAD^+ or NADP^+ . The activity with NADP^+ was more than 70x higher, indicating that isocitrate dehydrogenase is a relevant source of NADPH in *Accumulibacter*.

Additionally, the activity of other oxidoreductases and anaplerotic routes was measured: i) the reduction of oxaloacetate to malate (catalyzed by malate dehydrogenase) had, at least, 55x higher activity when using NADH

than NADPH. Because of the small activity observed when using NADPH, it was not possible to independently study the cofactor preference of the malic enzyme (oxidation of malate to pyruvate); ii) the glyoxylate shunt was also found to be active and to have an activity comparable to the positive biological control *E. coli* grown in acetate (well known to make use of the glyoxylate shunt (39)); and lastly, iii) fumarate reductase and α -ketoglutarate dehydrogenase were also tested but their activities were very low compared to all other enzymes tested in our study.

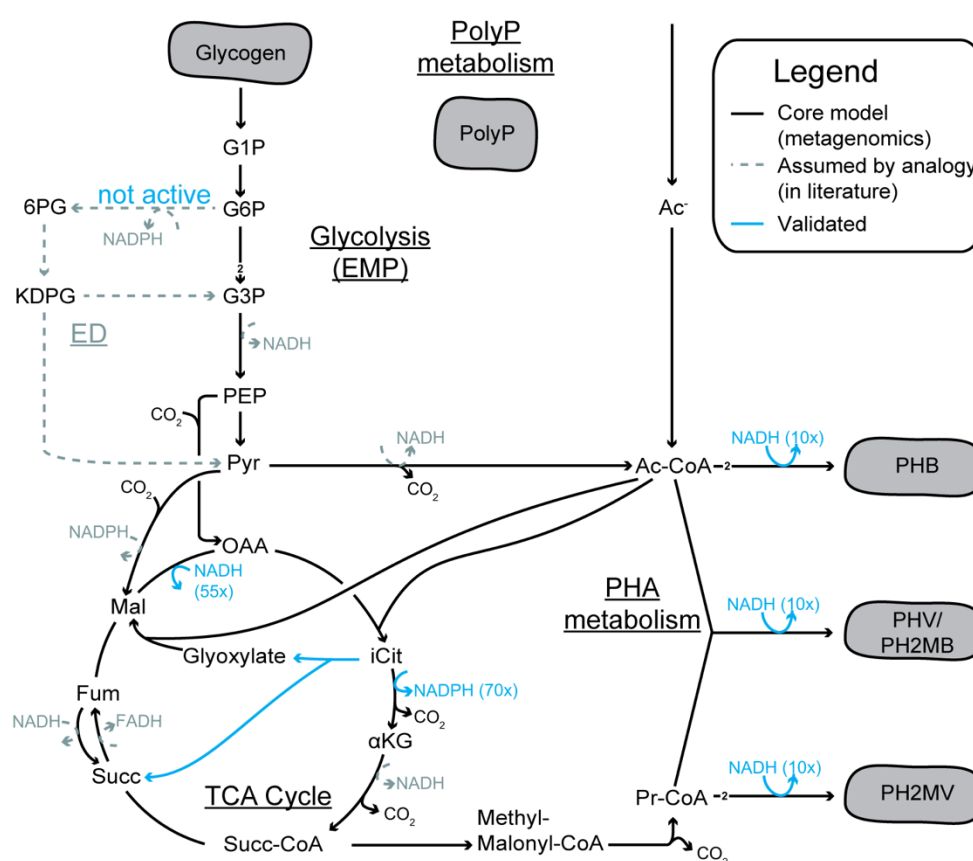


Figure 2 – Central carbon metabolic network of *Accumulibacter* including redox cofactor preference of oxidoreductases assayed in this study. A simplified version of this network (Table 3) was used for the simulations. The values shown corresponds to the factor difference between the preferred cofactor and the alternative one. This metabolic network is based on the ancestral genome reconstruction done by (2). The arrows show the expected flux direction under anaerobic conditions. The untested cofactor preferences (in gray) remain as assumed by analogy with other microorganisms. Despite not being annotated in the genome, the ED pathway has been suggested as the route for glycogen degradation (40, 41). A more extensive

overview of evidence for each pathway can be found in Supplementary Document S1. G1P, glucose-1-phosphate; G6P, glucose-6-phosphate; 6PG, 6-phosphogluconate; KDPG, 2-keto-3-deoxy-6-phosphogluconate; G3P, glyceraldehyde-3-phosphate; PEP, phosphoenolpyruvate; Pyr, pyruvate; OAA, oxaloacetate; Ac-CoA, Acetyl-CoA; iCit, isocitrate; α KG, α -ketoglutarate; Succ-CoA, succinyl-CoA; Succ, succinate; Fum, fumarate; Mal, malate; Pr-CoA, propionyl-CoA; Ac⁻, acetate; EMP, Embden-Meyerhof-Parnas; TCA, tricarboxylic acid cycle.

Anaerobic stoichiometric model construction

Based on the defined reaction network (Figure 2 and Table 3) the balance of reducing equivalents by *Accumulibacter* during anaerobic acetate conversion to PHAs was studied quantitatively. Note that the network from Figure 2 was further simplified (Table 3) based on the presented evidence that PHA accumulation in *Accumulibacter* is NADH-consuming rather than previously assumed NADPH preference based on genome annotations. The cofactor NADH can be regenerated from other electron carriers like NADPH or ferredoxin using transhydrogenases without any energetic cost for the cell (20).

This is not the case for FADH, which would require an input of energy (ATP) to be re-oxidized using NAD⁺. Currently, there is still no experimentally validated mechanism on how *Accumulibacter* could re-oxidize FADH in the absence of an external electron acceptor (e.g. oxygen or nitrate). Therefore, for this simulation, we blocked this FADH producing step in the TCA cycle (i.e. Succ-CoA to Fum) and for the remaining reactions we neglected the different types of redox cofactors by simply balancing “electrons” (note that each redox cofactor carries 2 electrons and, in some publications, these are simply referred to as [H]). Since the FADH producing step in the TCA cycle is blocked, only the oxidative branch (OAA to Succ-CoA via ICDH and AKGDH) and/or the reductive branch (OAA to Succ-CoA via MDH and FR) are possible.

374 Table 3 – Stoichiometry used for flux balance analysis (in mol basis) to simulate
 375 Accumulibacter's anaerobic metabolism. Reversible reaction: \leftrightarrow , irreversible reaction: \rightarrow . Note
 376 that these are lumped reactions, and each may involve several enzymatic steps. A
 377 comprehensive overview of the physiological studies published on Accumulibacter supporting
 378 this stoichiometric model can be found in the Supplementary Document S1.

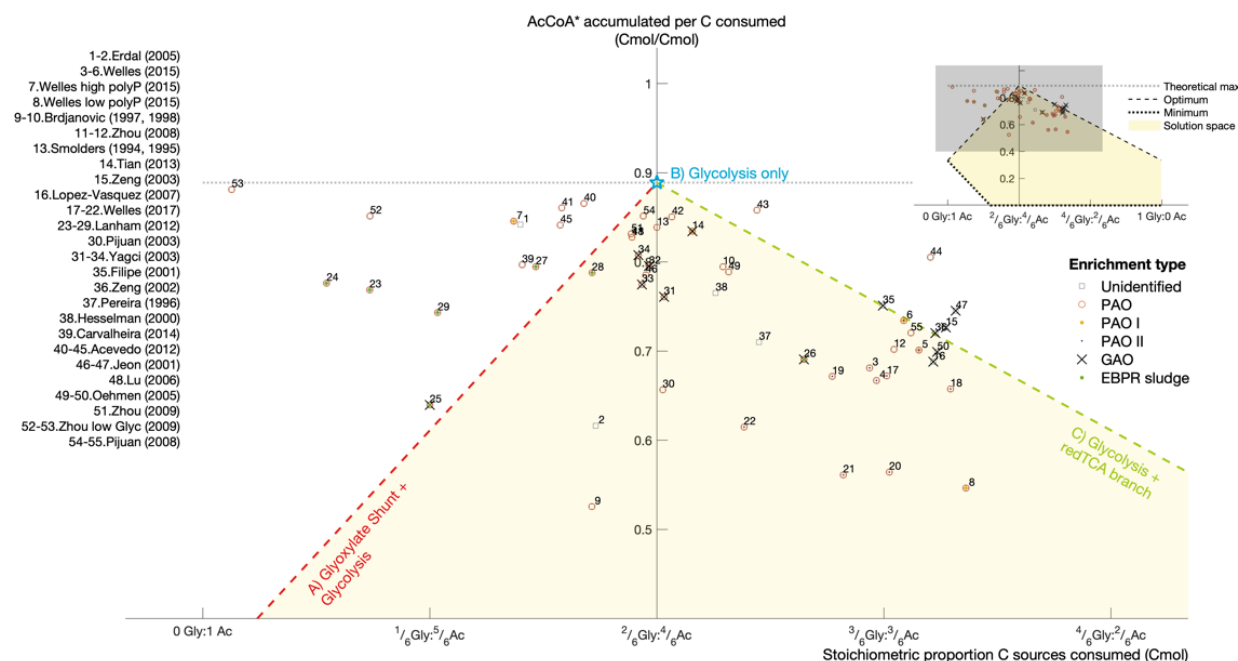
Pathway	Stoichiometry	Enzyme assayed in this study
Glycolysis (EMP)	$(\text{Glycogen})_1 \rightarrow 2 \text{ Pyr} + 4 \text{ electrons}$	G6PDH
Pyruvate to Acetyl-CoA	$\text{Pyr} \rightarrow \text{Ac-CoA} + 2 \text{ electrons} + \text{CO}_2$	
Pyruvate to Oxaloacetate	$\text{Pyr} + \text{CO}_2 \leftrightarrow \text{OAA}$	
Oxidative TCA branch	$\text{OAA} + \text{Ac-CoA} \rightarrow \text{Succ-CoA} +$ $2 \text{ CO}_2 + 4 \text{ electrons}$	ICDH AKGDH
Reductive TCA branch (reverse TCA)	$\text{OAA} + 4 \text{ electrons} \rightarrow \text{Succ-CoA}$	MDH FR
Glyoxylate shunt	$2 \text{ Ac-CoA} \rightarrow \text{Succ-CoA} + 2 \text{ electrons}$	ICL
Succinate-propionate shunt	$\text{Succ-CoA} \leftrightarrow \text{Pr-CoA} + \text{CO}_2$	
Ac-CoA* production (precursor for 3HB, 3HV and 3HMB)	$\text{Ac-CoA} + \text{electron} \rightarrow \text{Ac-CoA}^*$ (* means "+1electron")	AcAc-CoA red
Pr-CoA* production (precursor for 3H2MV, 3HV and 3HMB)	$\text{Pr-CoA} + \text{electron} \rightarrow \text{Pr-CoA}^*$ (* means "+1electron")	AcAc-CoA red

379
 380 In contrast to electron balances, the ATP balance cannot be used as there
 381 are still too many unknowns: 1) how much ATP can be generated from efflux of
 382 ions (potassium, magnesium and phosphate) associated with polyphosphate
 383 hydrolysis; 2) how much ATP is required for acetate uptake; 3) how much is

needed to upgrade redox cofactors (i.e. transfer electrons from low to high potential cofactors); 4) and how much ATP is used for cellular maintenance. Therefore, ATP is not balanced in this simulation. Nevertheless, it is important to note that the different pathways used for redox balancing will lead to different levels of ATP generation. Thus, in cases of polyphosphate limitation, the metabolism could prefer pathways with higher ATP-yield.

Experiments show that the ratio between glycogen and acetate consumption by PAOs is variable, e.g. between high/low temperature (42) or polyphosphate/glycogen availability (37, 43, 44). To reflect this variability, simulations were performed for a range of acetate and glycogen mixtures ranging from only acetate to only glycogen and results were compared to experimental data reported in literature.

For the anaerobic sequestration of acetate as PHA, acetate needs to be reduced (Ac-CoA*). The Ac-CoA* optimum in Figure 3 corresponds to the situation in which most carbon is kept inside the cell. The required reducing power can come from either glycolysis (glycogen breakdown) or glyoxylate shunt (acetate oxidation) operation. The different modes are presented in Figure 4. These modes respectively form the extreme left and right values of the optimum line in Figure 3. If glycogen degradation can supply exactly the amount of electrons needed for the uptake and conversion of acetate, then only Ac-CoA* (as PHB) is produced and there is no need to use any part of the TCA cycle (Figure 4B, and highest PHB yield in Figure 3).



406

407

408

409

410

411

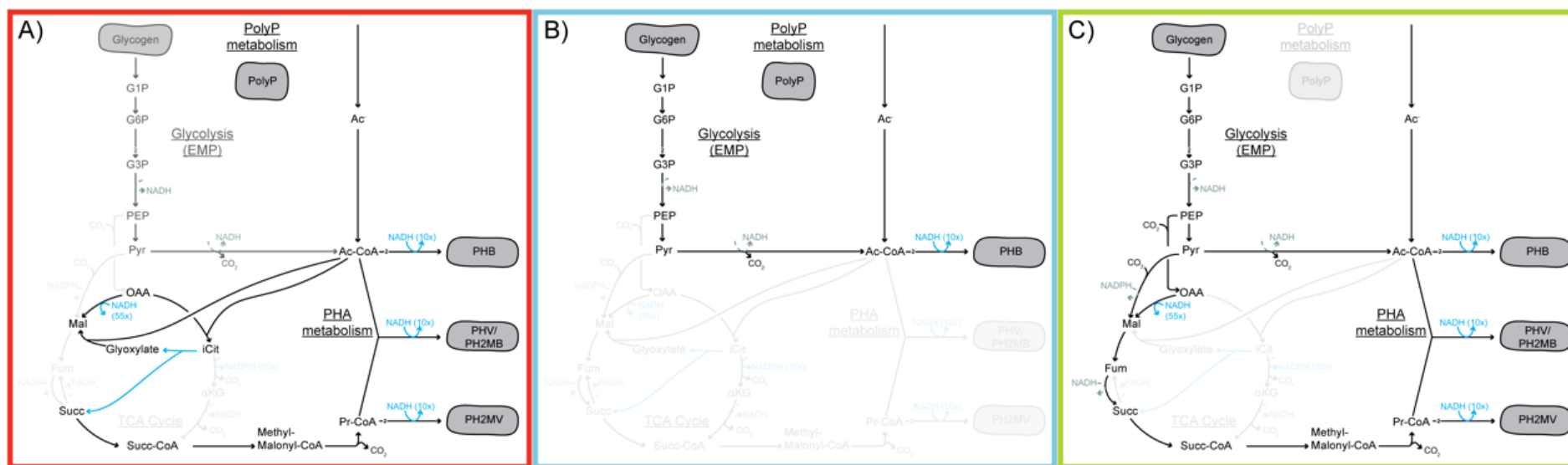
412

413

414

Figure 3 – The amount of Ac-CoA* accumulated (PHB and PHV precursor) depends on the different proportion of glycogen to acetate consumed and on the available pathways. The three optimum redox balancing strategies are shown in Figure 4 ABC. From 0 to approx. 2/6 glycogen Cmol, it can be considered that bacteria are performing a polyphosphate-based metabolism (PAM, optimum line in red) and from approx. 3/6 to 1 glycogen Cmol, a glycogen-based metabolism (GAM, optimum line in green) is used. The “optimum” and “minimum” lines were obtained by minimizing and maximizing CO₂ production, respectively. The feasible solution space (in yellow) lies in between these two cellular objectives, in which a mixture of different redox balancing strategies is used. The minimum carbon conserving strategy is the one that only uses the oxidative TCA branch. Experimental datasets were retrieved from (10, 37, 50–59, 41, 42, 44–49) and normalized to respect carbon and energy conservation principles (see Supplementary Document S5). Similar plots for Pr-CoA*, CO₂, alternative simulations and including error bars on the experimental data points can be found in Supplementary Document S6.

415 The optimum can probably only be achieved with polyphosphate as ATP
 416 source. In a typical GAO-like metabolism, an excess of glycogen is degraded
 417 compared to the acetate consumed to supply all ATP needed. This leads to the
 418 generation of an excess of reducing power, which is used to produce Pr-CoA*
 419 leading to PHAs more reduced than PHB (e.g. PHV or PH2MV), using the
 420 reductive TCA branch (Figure 4C). On the other hand, in a PAO-like metabolism
 421 the amount of reducing equivalents generated by glycolysis is usually lower
 422 than required to reduce all consumed acetate. In this situation, part of the
 423 acetate is oxidized to produce reducing equivalents. Such oxidation is possible
 424 via an active glyoxylate shunt which was also found from the enzymatic assays.
 425 The simulations show this as the optimal pathway to produce PHAs when
 426 glycogen is limiting (Figure 4A), i.e. it allows for higher carbon conservation (i.e.
 427 higher PHA yield) than the “horseshoe” TCA operation.



428

429

430

431

432

433

Figure 4 – Different optimum redox balancing strategies for *Accumulibacter* under anaerobic conditions. A) When little glycogen is degraded and is not enough to reduce all acetate to PHB, the glyoxylate shunt as recommended by (55) is the most optimal way to provide these electrons. B) When the stoichiometric amount of glycogen is degraded for acetate reduction to PHB, there is no real need to operate any part of the TCA cycle to balance redox and only PHB is then produced, as proposed in (60). C) When more glycogen than needed for acetate reduction is degraded, the reductive TCA branch can be used as proposed by (55) for GAOs to sink electrons in more reduced PHAs (e.g. PHV and PH2MV).

DISCUSSION

Characterization of *Accumulibacter* enrichments

The discussion will be based on the observed high PAO enrichment of mainly *Ca. Accumulibacter phosphatis* clade I. Consequently, extrapolations of these results to *Accumulibacter* clade II or GAOs are speculative until further validation using respective environments for enrichments (10, 47, 61–64).

Updated biochemical (stoichiometric) model

The presented study shows that the metabolic traits of *Accumulibacter* enable a flexible metabolic operation under anaerobic conditions. This flexibility is made possible by their energy and reducing power storage, enabling the observed phenotypes: fast anaerobic acetate uptake and anaerobic PHB synthesis (decoupled from growth). The flexible reducing power balancing by *Accumulibacter* depends on the nature of the redox cofactors used – here, enzymatic assays were performed to define the redox cofactor preferences of the main oxidoreductases in the central metabolic pathways of *Accumulibacter*.

The key finding from these assays is the NADH-preferring PHA accumulation in *Accumulibacter*. This NADH-preference allows for a direct consumption of the NADH produced in most of *Accumulibacter*'s reducing power sources. This also eliminates the need for NADH into NADPH conversion, which was suggested earlier by (11) using the membrane-bound transhydrogenase (PntAB) driven by proton motive force. Although there are previous reports showing NADH-driven PHB accumulation (13, 65–68), the level of NADH preference of the acetoacetyl-CoA reductase from *Accumulibacter* is striking. Further characterization of this enzyme was undertaken by Olavarria and

colleagues (in preparation). This observation allows to re-think the role of PHAs: we hypothesize that depending on the environment where microorganisms thrive, PHA accumulation will play a role as carbon reservoir during metabolic over-flow (NADPH-driven accumulation) or as an electron reservoir during scarcity of external electron acceptors (NADH-driven accumulation). Thus, for *Accumulibacter*, PHA is essentially a fermentation product.

A related finding was the absence of activity of the first step of the sometimes-implicated ED glycolytic pathway. These results match those observed by (42) and in (69) for GAOs, where no NADP⁺ dependent glucose-6-phosphate dehydrogenase activity was found. The experimental findings are in line with the absence of key ED genes in the genome annotations of *Accumulibacter* and closest relatives *Dechloromonas aromatica* and *Azoarcus* sp. *EbN1* (64, 70). Furthermore, no enzymatic activity of the ED pathway with NAD⁺ as electron acceptor (38) was observed.

These findings are in contradiction with earlier ¹³C NMR studies (40, 41), which indicated that the ED pathway was more likely the route for glycolysis than EMP. Nevertheless, it has to be noted that these early studies comprise interpretations of ¹³C patterns using simplified metabolic models, with limited information on the reversibility of each reaction and potentially with reactions missing; these are common pitfalls of the ¹³C-labelling method (71). Also note that these ¹³C NMR studies were performed before the first draft genome of *Accumulibacter* was available (70), and only the ¹³C pattern in the different PHAs was measured and not in the metabolic intermediates of each pathway used.

While NADPH is not required anaerobically by *Accumulibacter*, this reducing cofactor has to be produced aerobically to drive biomass synthesis. Here, isocitrate dehydrogenase was found NADP⁺ dependent. This is consistent with the observation that most acetate consumers will use this conversion to produce NADPH for their anabolism (72) and confirms the protein annotation found in (64). Since PHA accumulation is now known to be NADH-preferring and without another sink of NADPH, the latter might accumulate anaerobically and thereby inhibit the isocitrate dehydrogenase reaction. Alternatively, a soluble transhydrogenase could convert this NADPH into NADH and allow the oxidative branch of the TCA to be operational under anaerobic conditions.

Regarding the activity of other TCA oxidoreductases and anaplerotic routes: i) the oxidation of malate using NAD⁺ was also found in the studies of (42); ii) the glyoxylate shunt was also found active as observed in assays done by (41, 42, 73) and metatranscriptomics/proteomics studies by (2, 63, 74–76), which is expected as this is the anaplerotic route that allows for microorganisms to convert C2 sources like acetate into C4 building blocks for anabolism (72); and iii) fumarate reductase and α -ketoglutarate dehydrogenase activities were very low compared to all other enzymes tested in our study and alike in the studies of (42). An α -ketoglutarate:ferredoxin oxidoreductase has been identified in *Accumulibacter*'s genome and proteome (64). This has not been assayed here as sufficient evidence was collected suggesting an anaerobic operation mode via the glyoxylate shunt rather than a full or partial oxidative TCA cycle.

Flexible anaerobic metabolism – Adjustments depending on the environment and intracellular storage compounds

As (9) suggested in their review, the flexibility of *Accumulibacter*'s metabolism is likely the major reason why there is controversy in literature regarding how reducing power is balanced under anaerobic conditions. Long-term exposure to set conditions (e.g. pH, temperature, oxidation level of the substrate, nutrient availability, counter-ions, SRT, settling time) will select for the best strategy for those conditions, but short-term perturbations of those set conditions have shown that *Accumulibacter* seems to still be able to solve the redox balancing problem even if sub-optimally regarding carbon conservation (10, 43, 44, 77). Thus, based on our analysis, we observe that there is not one fixed stoichiometry, but a range of possible stoichiometries that in the end are defined by the relative proportions of each of the intervening substrates, supplied to the system or produced by a side-population (e.g. acetate, glycogen, polyphosphate, other VFAs, oxygen, nitrate, hydrogen).

The simulations showed *Accumulibacter* can operate in three distinct modes (and combinations in between): A) when reducing equivalents from glycolysis are limiting compared to the acetate imported (Yagci's model (55)); B) when glycolysis supplies exactly enough reducing equivalents to convert all imported acetate into PHB (Mino's model (60)); and lastly C) when glycolysis is producing an excess of reducing equivalents (alike Yagci's model for GAOs (55)).

The anaerobic use of the glyoxylate shunt in a PAO-like metabolism to provide for the reducing equivalents needed for PHA accumulation is supported by the studies of (55, 73); However, as seen in Figure 3, it does not explain the higher levels of Ac-CoA* found (points above the red optimum line) when a shift

to more reduced PHAs (Pr-CoA^{*}) was expected. This indicates that there might be an alternative process that allows the cell to conserve extra carbon, in other words, accumulate more Ac-CoA^{*} and less Pr-CoA^{*}. It could be that 1) fully anaerobic conditions were not attained when performing the experiments, or that 2) another side population is providing electrons in the form of a more reduced organic substrate or even hydrogen gas (78) or 3) *Accumulibacter* has yet another, alternative way of balancing redox which has yet to be described and demonstrated.

Also for the scenario where glycolysis produces an excess of reduced cofactors as in a GAO-like metabolism, a few experimental data points fall outside the feasible solution space (points above the green optimum line in Figure 3); these could be explained in the case that *Accumulibacter* produces H₂ to solve an excess of NADH as described by (11).

The multilayered complexity of a physiological analysis of *Accumulibacter*

The experimental data gathered are likely also influenced by the intrinsic heterogeneity of *Accumulibacter* enrichments; clade differences, population heterogeneity or even different environment (e.g. depending on the position of the cell in a floc/granule). Therefore, experimental data points under the optimum line in Figure 3 likely represent mixtures of cells, each with a different metabolic mode (Figure 4 A, B or C). Furthermore, any kinetic limitation (i.e. pathway capacity) may also explain a sub-optimal, mixed phenotype.

Additionally, if all enzymatic machinery is available, it seems possible that the same cell might change modes depending on the environment and its intracellular storage dynamics. Particularly, availability of acetate (e.g.

transition feast/famine) and/or polyphosphate storage as well as glycogen can trigger shifts in metabolic mode.

Despite the heterogeneity and noise, the experimental data outside the solution space suggests this stoichiometric model is still incomplete to represent all experimental conditions. The solution space expands for example when (1) allowing for hydrogen production in excess glycogen-to-acetate conditions or (2) the oxidation of acetate in a fully operational TCA cycle in a glycolysis-limiting scenario. With these reactions, all experimental data can be explained (see Supplementary Document S6). The first is supported by the detection of hydrogen gas produced by an *Accumulibacter* enrichment (11). For the latter, a full TCA cycle has been previously suggested based on ^{13}C NMR observations (58) and stoichiometric analyses by (43). Additionally, a novel protein has been proposed based on metagenomic analysis that could allow for full TCA operation under anaerobic conditions (70); however, there is still no direct biochemical experimental evidence that indeed validates a full anaerobic TCA operation. Some indirect observation is presented in (79). Here, labelled propionate was used as substrate and ^{13}C enrichment was found in the PHV fragments that come from acetyl-CoA. This labeling pattern can be explained by a full TCA, but this is not the only metabolic route that could explain this observation.

Alternatively, it should also be considered that, alike many (strict) anaerobes, *Accumulibacter* may use electron bifurcation mechanisms (80) via ferredoxin oxidoreductases to allow for alternative pathways in the central carbon metabolism.

CONCLUSION

In this study a network-based modeling approach was used to unravel the metabolic flexibility of *Accumulibacter* under dynamic conditions. The approach integrates findings and hypotheses derived from previous meta-omics studies as well as different physiological datasets and biochemical assays.

The developed metabolic model demonstrates the flexibility in metabolic function and could explain previous controversy in PAO literature. The NADH dependent PHA synthesis is both an efficient link to catabolic pathways as well as key for enabling metabolic flexibility. Depending on the exact history and cultivation conditions, *Accumulibacter* can exhibit different metabolic phenotypes; the metabolic network can handle different combinations of carbon sources (i.e. acetate and glycogen) adjusting the use of glycolysis (EMP), different branches of the TCA cycle (incl. glyoxylate shunt) and potentially other pathways not yet considered. This poses a challenge to predictive EBPR modeling, as this implies that stoichiometry is not fixed, but variable, spanning continuously from polyphosphate to glycogen-based phenotypes.

This metabolic versatility is likely what allows *Accumulibacter* to be, in most situations, very close to a carbon conservation optimum, which is key to ensure their competitiveness in the dynamic environments of EBPR systems.

599 **ACKNOWLEDGEMENTS**

600 These investigations were supported by the SIAM Gravitation Grant
 601 024.002.002, the Netherlands Organization for Scientific Research (NWO). The
 602 authors would like to thank Roel van de Wijngaart, Alexandre Carnet, Hein van
 603 der Wall, Koen Verhagen, David Weissbrodt, Alex Salazar, and Thomas Abeel
 604 for their collaboration in this project. The authors would also like to thank to
 605 Sergio Tomás Martínez and Eleni Vasilakou for proofreading and Ben
 606 Oyserman for his invaluable advice on this manuscript.

607 **COMPETING INTERESTS**

608 The authors declare no conflict of interest.

609 REFERENCES

- 610 1. Van Loosdrecht MCM, Pot M a., Heijnen JJ. 1997. Importance of bacterial storage
611 polymers in bioprocesses. *Water Sci Technol* 35:41–47.
- 612 2. Oyserman BO, Moya F, Lawson CE, Garcia AL, Vogt M, Heffernan M, Noguera DR,
613 McMahon KD. 2016. Ancestral genome reconstruction identifies the evolutionary
614 basis for trait acquisition in polyphosphate accumulating bacteria. *ISME J* 10:2931–
615 2945.
- 616 3. McMahon KD, Read EK. 2013. Microbial contributions to phosphorus cycling in
617 eutrophic lakes and wastewater. *Annu Rev Microbiol* 67:199–219.
- 618 4. Seviour RJ, Mino T, Onuki M. 2003. The microbiology of biological phosphorus
619 removal in activated sludge systems. *FEMS Microbiol Rev* 27:99–127.
- 620 5. Barnard JL. 1976. A review of Biological Phosphorous Removal in the Activated
621 Sludge Process. *Water Sa* 2:136–144.
- 622 6. Seviour RJ, Mclroy S. 2008. The microbiology of phosphorus removal in activated
623 sludge processes-the current state of play. *J Microbiol* 46:115–124.
- 624 7. Mino T, van Loosdrecht MCM, Heijnen JJ. 1998. Microbiology and biochemistry of
625 the enhanced biological phosphate removal process. *Water Res* 32:3193–3207.
- 626 8. Oehmen A, Lemos PC, Carvalho G, Yuan Z, Keller J, Blackall LL, Reis M a M. 2007.
627 Advances in enhanced biological phosphorus removal: From micro to macro scale.
628 *Water Res* 41:2271–2300.
- 629 9. Zhou Y, Pijuan M, Oehmen A, Yuan Z. 2010. The source of reducing power in the
630 anaerobic metabolism of polyphosphate accumulating organisms (PAOs) - A mini-
631 review. *Water Sci Technol* 61:1653–1662.
- 632 10. Welles L, Tian WD, Saad S, Abbas B, Lopez-Vazquez CM, Hooijmans CM, van
633 Loosdrecht MCM, Brdjanovic D. 2015. Accumulibacter clades Type I and II
634 performing kinetically different glycogen-accumulating organisms metabolisms for
635 anaerobic substrate uptake. *Water Res* 83:354–366.
- 636 11. Oyserman BO, Noguera DR, del Rio TG, Tringe SG, McMahon KD. 2016.
637 Metatranscriptomic insights on gene expression and regulatory controls in
638 Candidatus Accumulibacter phosphatis. *ISME J* 10:810–22.
- 639 12. Madison LL, Huisman GW. 1999. Metabolic Engineering of Poly (3-
640 Hydroxyalkanoates): From DNA to Plastic. *Microbiol Mol Biol Rev* 63:21–53.
- 641 13. Ritchie GAF, Senior PJ, Dawes EA. 1971. The Purification and Characterization of
642 Acetoacetyl-Coenzyme A Reductase from *Azotobacter beijerinckii*. *Biochem J*
643 121:309–316.
- 644 14. Senior PJ, Beech GA, Ritchie GA, Dawes EA. 1972. The role of oxygen limitation
645 in the formation of poly- -hydroxybutyrate during batch and continuous culture of
646 *Azotobacter beijerinckii*. *Biochem J* 128:1193–201.
- 647 15. Liebergesell M, Steinbüchel A. 1992. Cloning and nucleotide sequences of genes
648 relevant for biosynthesis of poly(3-hydroxybutyric acid) in *Chromatium vinosum*
649 strain D. *Eur J Biochem* 209:135–50.
- 650 16. Satoh Y, Tajima K, Tannai H, Munekata M. 2003. Enzyme-catalyzed poly(3-
651 hydroxybutyrate) synthesis from acetate with CoA recycling and NADPH
652 regeneration in Vitro. *J Biosci Bioeng* 95:335–341.
- 653 17. Chohan, Copeland. 1998. Acetoacetyl coenzyme A reductase and
654 polyhydroxybutyrate synthesis in rhizobium (Cicer) sp. Strain CC 1192. *Appl*
655 *Environ Microbiol* 64:2859–63.
- 656 18. Olavarria K, Marone MP, da Costa Oliveira H, Roncallo JC, da Costa Vasconcelos
657 FN, da Silva LF, Gomez JGC. 2015. Quantifying NAD(P)H production in the upper

- 658 Entner-Doudoroff pathway from *Pseudomonas putida* KT2440. *FEBS Open Bio*
659 5:908–15.
- 660 19. Dean AM, Golding GB. 1997. Protein engineering reveals ancient adaptive
661 replacements in isocitrate dehydrogenase. *Proc Natl Acad Sci U S A* 94:3104–9.
- 662 20. Fuhrer T, Sauer U. 2009. Different biochemical mechanisms ensure network-wide
663 balancing of reducing equivalents in microbial metabolism. *J Bacteriol* 191:2112–
664 2121.
- 665 21. Bologna FP, Andreo CS, Drincovich MF. 2007. *Escherichia coli* malic enzymes: two
666 isoforms with substantial differences in kinetic properties, metabolic regulation, and
667 structure. *J Bacteriol* 189:5937–46.
- 668 22. Giachetti E, Pinzauti G, Vanni P. 1984. A new continuous optical assay for isocitrate
669 lyase. *Experientia* 40:227–228.
- 670 23. Hillier AJ, Jericho RE, Green SM, Jago GR. 1979. Properties and function of
671 fumarate reductase (NADH) in *Streptococcus lactis*. *Aust J Biol Sci* 32:625–35.
- 672 24. Bunik VI, Denton TT, Xu H, Thompson CM, Cooper AJL, Gibson GE. 2005.
673 Phosphonate Analogues of α -Ketoglutarate Inhibit the Activity of the α -Ketoglutarate
674 Dehydrogenase Complex Isolated from Brain and in Cultured Cells †. *Biochemistry*
675 44:10552–10561.
- 676 25. Daims H, Brühl A, Amann R, Schleifer KH, Wagner M. 1999. The domain-specific
677 probe EUB338 is insufficient for the detection of all Bacteria: development and
678 evaluation of a more comprehensive probe set. *Syst Appl Microbiol* 22:434–44.
- 679 26. Amann RI. 1995. In situ identification of micro-organisms by whole cell hybridization
680 with rRNA-targeted nucleic acid probes, p. 331–345. *In* Akkermans, ADL, Van
681 Elsas, JD, De Bruijn, FJ (eds.), *Molecular Microbial Ecology Manual*. Springer
682 Netherlands, Dordrecht.
- 683 27. Amann RI, Binder BJ, Olson RJ, Chisholm SW, Devereux R, Stahl DA. 1990.
684 Combination of 16S rRNA-targeted oligonucleotide probes with flow cytometry for
685 analyzing mixed microbial populations. *Appl Environ Microbiol* 56:1919–25.
- 686 28. Flowers JJ, He S, Yilmaz S, Noguera DR, McMahon KD. 2009. Denitrification
687 capabilities of two biological phosphorus removal sludges dominated by different
688 “*Candidatus Accumulibacter*” clades. *Environ Microbiol Rep* 1:583–588.
- 689 29. Rubio-Rincón FJ, Welles L, Lopez-Vazquez CM, Nierychlo M, Abbas B, Geleijnse
690 M, Nielsen PH, van Loosdrecht MCM, Brdjanovic D. 2017. Long-term effects of
691 sulphide on the enhanced biological removal of phosphorus: The symbiotic role of
692 *Thiothrix caldifontis*. *Water Res* 116:53–64.
- 693 30. Saad SA, Welles L, Abbas B, Lopez-Vazquez CM, van Loosdrecht MCM,
694 Brdjanovic D. 2016. Denitrification of nitrate and nitrite by ‘*Candidatus*
695 *Accumulibacter phosphatis*’ clade IC. *Water Res* 105:97–109.
- 696 31. McMahon KD, Yilmaz S, He S, Gall DL, Jenkins D, Keasling JD. 2007.
697 Polyphosphate kinase genes from full-scale activated sludge plants. *Appl Microbiol*
698 *Biotechnol* 77:167–173.
- 699 32. Schloss PD, Westcott SL, Ryabin T, Hall JR, Hartmann M, Hollister EB, Lesniewski
700 RA, Oakley BB, Parks DH, Robinson CJ, Sahl JW, Stres B, Thallinger GG, Horn DJ
701 Van, Weber CF. 2009. Introducing mothur: Open-Source, Platform-Independent,
702 Community-Supported Software for Describing and Comparing Microbial
703 Communities. *Appl Environ Microbiol* 75:7537–7541.
- 704 33. Caporaso JG, Kuczynski J, Stombaugh J, Bittinger K, Bushman FD, Costello EK,
705 Fierer N, Peña AG, Goodrich JK, Gordon JL, Huttley G a, Kelley ST, Knights D,
706 Koenig JE, Ley RE, Lozupone C a, McDonald D, Muegge BD, Pirrung M, Reeder J,
707 Sevinsky JR, Turnbaugh PJ, Walters W a, Widmann J, Yatsunenko T, Zaneveld J,
708 Knight R. 2010. QIIME allows analysis of high-throughput community sequencing

- 709 data. *Nat Methods* 7:335–6.
- 710 34. Quast C, Pruesse E, Yilmaz P, Gerken J, Schweer T, Yarza P, Peplies J, Glöckner
711 FO. 2013. The SILVA ribosomal RNA gene database project: improved data
712 processing and web-based tools. *Nucleic Acids Res* 41:D590-6.
- 713 35. Orth JD, Thiele I, Palsson BØ. 2010. What is flux balance analysis? *Nat Biotechnol*
714 28:245–8.
- 715 36. van der Heijden RTJM, Heijnen JJ, Hellinga C, Romein B, Luyben KCAM. 1994.
716 Linear constraint relations in biochemical reaction systems: I. Classification of the
717 calculability and the balanceability of conversion rates. *Biotechnol Bioeng* 43:3–10.
- 718 37. Welles L, Abbas B, Sorokin DY, Lopez-Vazquez CM, Hooijmans CM, van
719 Loosdrecht MCM, Brdjanovic D. 2017. Metabolic response of “candidatus
720 *accumulibacter phosphatis*” clade II C to changes in influent P/C ratio. *Front*
721 *Microbiol* 7.
- 722 38. Olavarria K, Valdés D, Cabrera R. 2012. The cofactor preference of glucose-6-
723 phosphate dehydrogenase from *Escherichia coli*—modeling the physiological
724 production of reduced cofactors. *FEBS J* 279:2296–309.
- 725 39. Gottschalk G. 1986. *Bacterial Metabolism*. Springer New York, New York, NY.
- 726 40. Maurer M, Gujer W, Hany R, Bachmann S. 1997. Intracellular carbon flow in
727 phosphorus accumulating organisms from activated sludge systems. *Water Res*
728 31:907–917.
- 729 41. Hesselmann RPX, Von Rummell R, Resnick SM, Hany R, Zehnder a. JB. 2000.
730 Anaerobic metabolism of bacteria performing enhanced biological phosphate
731 removal. *Water Res* 34:3487–3494.
- 732 42. Erdal ZK, Erdal UG, Randall CW. 2005. Biochemistry of enhanced biological
733 phosphorus removal and anaerobic COD stabilization. *Water Sci Technol* 52:557–
734 567.
- 735 43. Zhou Y, Pijuan M, Zeng RJ, Yuan Z. 2009. Involvement of the TCA cycle in the
736 anaerobic metabolism of polyphosphate accumulating organisms (PAOs). *Water*
737 *Res* 43:1330–1340.
- 738 44. Zhou Y, Pijuan M, Zeng RJ, Lu H, Yuan Z. 2008. Could polyphosphate-
739 accumulating organisms (PAOs) be glycogen-accumulating organisms (GAOs)?
740 *Water Res* 42:2361–2368.
- 741 45. Brdjanovic D, Loosdrecht MCM van, Hooijmans CM, Alaerts GJ, Heijnen JJ. 1997.
742 Temperature Effects on Physiology of Biological Phosphorus Removal. *J Environ*
743 *Eng* 123:144–153.
- 744 46. Brdjanovic D, Van Loosdrecht MCM, Hooijmans CM, Mino T, Alaerts GJ, Heijnen
745 JJ. 1998. Effect of polyphosphate limitation on the anaerobic metabolism of
746 phosphorus-accumulating microorganisms. *Appl Microbiol Biotechnol* 50:273–276.
- 747 47. Acevedo B, Oehmen A, Carvalho G, Seco a., Borrás L, Barat R. 2012. Metabolic
748 shift of polyphosphate-accumulating organisms with different levels of
749 polyphosphate storage. *Water Res* 46:1889–1900.
- 750 48. Smolders GJF, van der Meij J, van Loosdrecht MCM, Heijnen JJ. 1994.
751 Stoichiometric model of the aerobic metabolism of the biological phosphorus
752 removal process. *Biotechnol Bioeng* 44:837–848.
- 753 49. Smolders GJF, Klop JM, van Loosdrecht MCM, Heijnen JJ. 1995. A metabolic
754 model of the biological phosphorus removal process: I. Effect of the sludge retention
755 time. *Biotechnol Bioeng* 48:222–233.
- 756 50. Tian W-D, Lopez-Vazquez CM, Li W-G, Brdjanovic D, van Loosdrecht MCM. 2013.
757 Occurrence of PAOI in a low temperature EBPR system. *Chemosphere* 92:1314–
758 20.

- 759 51. Zeng RJ, Yuan Z, Keller J. 2003. Model-based analysis of anaerobic acetate uptake
760 by a mixed culture of polyphosphate-accumulating and glycogen-accumulating
761 organisms. *Biotechnol Bioeng* 83:293–302.
- 762 52. López-Vázquez CM, Hooijmans CM, Brdjanovic D, Gijzen HJ, van Loosdrecht
763 MCM. 2007. A practical method for quantification of phosphorus- and glycogen-
764 accumulating organism populations in activated sludge systems. *Water Environ Res*
765 79:2487–2498.
- 766 53. Lanham AB. 2012. Full-scale biological phosphorus removal: quantification of
767 storage polymers, microbial performance and metabolic modelling. Universidade
768 Nova de Lisboa.
- 769 54. Pijuan M, Saunders AM, Guisasola A, Baeza JA, Casas C, Blackall LL. 2004.
770 Enhanced biological phosphorus removal in a sequencing batch reactor using
771 propionate as the sole carbon source. *Biotechnol Bioeng* 85:56–67.
- 772 55. Yagci N, Artan N, Çokgör EU, Randall CW, Orhon D. 2003. Metabolic model for
773 acetate uptake by a mixed culture of phosphate- and glycogen-accumulating
774 organisms under anaerobic conditions. *Biotechnol Bioeng* 84:359–373.
- 775 56. Filipe CDM, Daigger GT, Grady CPL. 2001. A metabolic model for acetate uptake
776 under anaerobic conditions by glycogen accumulating organisms: Stoichiometry,
777 kinetics, and the effect of pH. *Biotechnol Bioeng* 76:17–31.
- 778 57. Zeng R, Yuan Z, van Loosdrecht MCM, Keller J. 2002. Proposed modifications to
779 metabolic model for glycogen-accumulating organisms under anaerobic conditions.
780 *Biotechnol Bioeng* 80:277–279.
- 781 58. Pereira H, Lemos PC, Reis MAM, Crespo JPSG, Carrondo MJT, Santos H. 1996.
782 Model for carbon metabolism in biological phosphorus removal processes based on
783 in vivo ¹³C-NMR labelling experiments. *Water Res* 30:2128–2138.
- 784 59. Carvalheira M. 2014. The effect of key process operational conditions on enhanced
785 biological phosphorus removal from wastewater. Universidade Nova de Lisboa.
- 786 60. Mino T, Tsuzuki Y, Matsuo T. 1987. Effect of phosphorus accumulation on acetate
787 metabolism in the biological phosphorus removal process, p. 27–38. *In* Ramadori,
788 R (ed.), *Biological phosphate removal from wastewaters: proceedings from the*
789 *International Conference of Advanced Water Pollution Control (IAWPRC)*.
790 Pergamon Press, Oxford, England.
- 791 61. Flowers JJ, He S, Malfatti S, del Rio TG, Tringe SG, Hugenholtz P, McMahon KD.
792 2013. Comparative genomics of two “*Candidatus Accumulibacter*” clades
793 performing biological phosphorus removal. *ISME J* 7:2301–14.
- 794 62. Welles L, Lopez-Vazquez CM, Hooijmans CM, van Loosdrecht MCM, Brdjanovic D.
795 2016. Prevalence of ‘*Candidatus Accumulibacter phosphatis*’ type II under
796 phosphate limiting conditions. *AMB Express* 6.
- 797 63. Wexler M, Richardson DJ, Bond PL. 2009. Radiolabelled proteomics to determine
798 differential functioning of *Accumulibacter* during the anaerobic and aerobic phases
799 of a bioreactor operating for enhanced biological phosphorus removal. *Environ*
800 *Microbiol* 11:3029–3044.
- 801 64. Barr JJ, Dutilh BE, Skennerton CT, Fukushima T, Hastie ML, Gorman JJ, Tyson
802 GW, Bond PL. 2016. Metagenomic and metaproteomic analyses of *Accumulibacter*
803 *phosphatis*-enriched floccular and granular biofilm. *Environ Microbiol* 18:273–87.
- 804 65. Kim J, Chang JH, Kim K-J. 2014. Crystal structure and biochemical properties of
805 the (S)-3- hydroxybutyryl-CoA dehydrogenase PaaH1 from *Ralstonia eutropha*.
806 *Biochem Biophys Res Commun* 448:163–168.
- 807 66. Barycki JJ, O LK, Strauss AW, Banaszak LJ, Author C, Banaszak Dietrich Professor
808 LJ. 2000. Sequestration of the Active Site by Interdomain Shifting: Crystallographic
809 and Spectroscopic Evidence for Distinct Conformations of L-3-Hydroxyacyl-CoA

810 Dehydrogenase Running Title: Human L-3-Hydroxyacyl-CoA Dehydrogenase. JBC
811 Pap Press Publ.

812 67. Haywood GW, Anderson AJ, Chu L, Dawes EA. 1988. The role of NADH- and
813 NADPH-linked acetoacetyl-CoA reductases in the poly-3-hydroxybutyrate
814 synthesizing organism *Alcaligenes eutrophus*. FEMS Microbiol Lett 52:264–259.

815 68. Ling C, Qiao G-Q, Shuai B-W, Olavarria K, Yin J, Xiang R-J, Song K-N, Shen Y-H,
816 Guo Y, Chen G-Q. 2018. Engineering NADH/NAD⁺ ratio in *Halomonas*
817 *bluephagenesis* for enhanced production of polyhydroxyalkanoates (PHA). Metab
818 Eng 49:275–286.

819 69. Filipe CDM, Daigger GT, Grady CPL. 2001. A metabolic model for acetate uptake
820 under anaerobic conditions by glycogen accumulating organisms: Stoichiometry,
821 kinetics, and the effect of pH. Biotechnol Bioeng 76:17–31.

822 70. García Martín H, Ivanova N, Kunin V, Warnecke F, Barry KW, McHardy AC, Yeates
823 C, He S, Salamov A a, Szeto E, Dalin E, Putnam NH, Shapiro HJ, Pangilinan JL,
824 Rigoutsos I, Kyrpides NC, Blackall LL, McMahon KD, Hugenholtz P. 2006.
825 Metagenomic analysis of two enhanced biological phosphorus removal (EBPR)
826 sludge communities. Nat Biotechnol 24:1263–1269.

827 71. Van Winden W, Verheijen P, Heijnen S. 2001. Possible pitfalls of flux calculations
828 based on ¹³C-labeling. Metab Eng 3:151–162.

829 72. Gottschalk G. 1986. Bacterial Metabolism. Springer New York, New York, NY.

830 73. Burow LC, Mabbett AN, Blackall LL. 2008. Anaerobic glyoxylate cycle activity during
831 simultaneous utilization of glycogen and acetate in uncultured *Accumulibacter*
832 enriched in enhanced biological phosphorus removal communities. ISME J 2:1040–
833 51.

834 74. Skennerton CT, Barr JJ, Slater FR, Bond PL, Tyson GW. 2015. Expanding our view
835 of genomic diversity in *Candidatus Accumulibacter* clades. Environ Microbiol
836 17:1574–1585.

837 75. Wilmes P, Andersson AF, Lefsrud MG, Wexler M, Shah M, Zhang B, Hettich RL,
838 Bond PL, VerBerkmoes NC, Banfield JF. 2008. Community proteogenomics
839 highlights microbial strain-variant protein expression within activated sludge
840 performing enhanced biological phosphorus removal. ISME J 2:853–864.

841 76. He S, McMahon KD. 2011. “*Candidatus Accumulibacter*” gene expression in
842 response to dynamic EBPR conditions. ISME J 5:329–340.

843 77. Erdal UG, Erdal ZK, Daigger GT, Randall CW. 2008. Is it PAO-GAO competition or
844 metabolic shift in EBPR system? Evidence from an experimental study. Water Sci
845 Technol 58:1329–34.

846 78. Lawson CE, Strachan BJ, Hanson NW, Hahn AS, Hall ER, Rabinowitz B, Mavinic
847 DS, Ramey WD, Hallam SJ. 2015. Rare taxa have potential to make metabolic
848 contributions in enhanced biological phosphorus removal ecosystems. Environ
849 Microbiol 17:4979–4993.

850 79. Lemos PC, Serafim LS, Santos MM, Reis M a M, Santos H. 2003. Metabolic
851 Pathway for Propionate Utilization by Phosphorus-Accumulating Organisms in
852 Activated Sludge: ¹³C Labeling and In Vivo Nuclear Magnetic Resonance. Appl
853 Environ Microbiol 69:241–251.

854 80. Buckel W, Thauer RK. 2013. Energy conservation via electron bifurcating ferredoxin
855 reduction and proton/Na⁺ translocating ferredoxin oxidation. Biochim Biophys Acta
856 - Bioenerg 1827:94–113.

857